Advances in Chemical Physics
Stuart A. Rice and Aaron R. Dinner, Series Editors

Advances in Chemical Physics

Volume 161

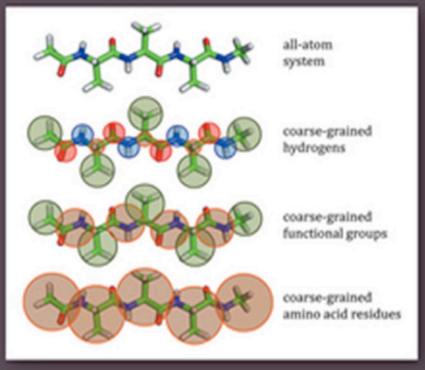

Edited by
Stuart A. Rice and Aaron R. Dinner

WILEY

ADVANCES IN CHEMICAL PHYSICS

VOLUME 161

ADVANCES IN CHEMICAL PHYSICS

VOLUME 161

Edited by

Stuart A. Rice

Department of Chemistry
and
The James Franck Institute,
The University of Chicago,
Chicago, IL, USA

Aaron R. Dinner

Department of Chemistry
and
The James Franck Institute,
The University of Chicago,
Chicago, IL, USA

WILEY

Published by John Wiley & Sons, Inc., Hoboken, New Jersey
Published simultaneously in Canada

Library of Congress Catalog Number: 58-9935

ISBN: 9781119290940

Set in 10/12pt Times by SPi Global, Pondicherry, India

Printed in the United States of America

10 9 8 7 6 5 4 3 2 1

EDITORIAL BOARD

CONTENTS

CONTRIBUTORS TO VOLUME 161

Massimo Altarelli, European XFEL GmbH, Schenefeld, Germany

William T. Coffey, Department of Electronic and Electrical Engineering, Trinity College, Dublin, Ireland

Jack F. Douglas, Materials Science and Engineering Division, National Institute of Standards and Technology, Gaithersburg, MD, USA

Karl F. Freed, James Franck Institute and Department of Chemistry, The University of Chicago, Chicago, IL, USA

Yuri P. Kalmykov, Laboratoire de Mathématiques et Physique (LAMPS, EA 4217), Université de Perpignan Via Domitia, Perpignan, France

John J. Kozak, Department of Chemistry, DePaul University, Chicago, IL, USA

Ruslan P. Kurta, European XFEL GmbH, Schenefeld, Germany

George D. J. Phillies, Department of Physics, Worcester Polytechnic Institute, Worcester, MA, USA

Jaroslaw Piasecki, Institute of Theoretical Physics, Faculty of Physics, University of Warsaw, Warsaw, Poland

M. Scott Shell, Department of Chemical Engineering, University of California Santa Barbara, Santa Barbara, CA, USA

Samanvaya Srivastava, Institute for Molecular Engineering, The University of Chicago, Chicago, IL, USA

Piotr Szymczak, Institute of Theoretical Physics, Faculty of Physics, University of Warsaw, Warsaw, Poland

Matthew V. Tirrell, Institute for Molecular Engineering, The University of Chicago, Chicago, IL, USA

Serguey V. Titov, Kotel'nikov Institute of Radio Engineering and Electronics of the Russian Academy of Sciences, Moscow, Russian Federation

Ivan A. Vartanyants, Deutsches Elektronen-Synchrotron, DESY, Hamburg, Germany; National Research Nuclear University 'MEPhI' (Moscow Engineering Physics Institute), Moscow, Russia

Wen-Sheng Xu, James Franck Institute, The University of Chicago, Chicago, IL, USA

PREFACE TO THE SERIES

Advances in science often involve initial development of individual specialized fields of study within traditional disciplines followed by broadening and overlap, or even merging, of those specialized fields, leading to a blurring of the lines between traditional disciplines. The pace of that blurring has accelerated in the past few decades, and much of the important and exciting research carried out today seeks to synthesize elements from different fields of knowledge. Examples of such research areas include biophysics and studies of nanostructured materials. As the study of the forces that govern the structure and dynamics of molecular systems, chemical physics encompasses these and many other emerging research directions. Unfortunately, the flood of scientific literature has been accompanied by losses in the shared vocabulary and approaches of the traditional disciplines, and there is much pressure from scientific journals to be ever more concise in the descriptions of studies, to the point that much valuable experience, if recorded at all, is hidden in supplements and dissipated with time. These trends in science and publishing make this series, *Advances in Chemical Physics*, a much needed resource.

The *Advances in Chemical Physics* is devoted to helping the reader obtain general information about a wide variety of topics in chemical physics, a field that we interpret very broadly. Our intent is to have experts present comprehensive analyses of subjects of interest and to encourage the expression of individual points of view. We hope that this approach to the presentation of an overview of a subject will both stimulate new research and serve as a personalized learning text for beginners in a field.

Stuart A. Rice
Aaron R. Dinner
January 2016, Chicago, IL, USA

STRUCTURAL ANALYSIS BY X-RAY INTENSITY ANGULAR CROSS CORRELATIONS

RUSLAN P. KURTA[1], MASSIMO ALTARELLI[1], and IVAN A. VARTANYANTS[2,3]

[1]European XFEL GmbH, Schenefeld, Germany
[2]Deutsches Elektronen-Synchrotron, DESY, Hamburg, Germany
[3]National Research Nuclear University 'MEPhI' (Moscow Engineering Physics Institute), Moscow, Russia

CONTENTS

Advances in Chemical Physics, Volume 161, First Edition. Edited by Stuart A. Rice and Aaron R. Dinner.

I. INTRODUCTION

The aim of this chapter is to review the topic of angular intensity correlations in X-ray diffraction. This topic has a history going back by almost 40 years, and is intertwined with developments in the related areas of intensity correlations in optical laser scattering and in electron scattering; but it has recently known a revival, partly related to the progress in X-ray sources and in instrumentation.

In the early literature, scattering experiments performed on randomly oriented objects in a solution were mostly discussed. Correlations between scattered intensity $I(\mathbf{q}, t)$ in different directions (for different scattering vectors $\mathbf{q}$) at the same or at different times t were considered,

$$C(\mathbf{q}_1, \mathbf{q}_2, t, t') \sim \langle I(\mathbf{q}_1, t) I(\mathbf{q}_2, t') \rangle, \tag{1}$$

where the brackets indicate an average over many measurements. In the case of light scattering [1, 2], a laser source was generally used and its full transverse coherence always implies an interference between the scattering by different particles inside the scattering volume. Also, rather large particles of the order of hundreds of nanometers, matching the wavelength of light, were investigated, in a concentration such that the average number of particles within the illuminated volume (defined by apertures) was rather small. The large particle size and the intensity of laser light combine to achieve an exposure time shorter than the characteristic orientational relaxation time of the objects. In the pioneering work by Kam [3], the intensity correlations between scattering of X-rays or neutrons from macromolecules in solution were addressed, also in the limit in which the data could be acquired in a time shorter than the characteristic molecular reorientation time. The possibility of this correlation analysis to obtain structural information without crystallization was proposed. Similar concepts were applied to electron microscopy; see, for example, Refs. 4 and 5.

The conventional X-ray scattering pattern of a disordered system, for example, a liquid, molecules in solution, or an amorphous solid is isotropic (Debye–Scherrer rings) when recorded with a weak, and low coherence, source [6, 7]. The weak source, in contrast to the previously discussed examples, means that the exposure time required to collect a sufficient signal, in the case of a liquid or a solution, is long compared to characteristic relaxation times of the rotational and translational agitation. If, on the other hand, the signal can be acquired in a short time with a brilliant X-ray source with a high degree of coherence, such as available with a third-generation synchrotron source or X-ray free-electron laser, the recorded pattern is not isotropic, but is an apparently random collection of speckles. These speckles are in fact encoding the instantaneous positions and orientations of the molecules. In an amorphous solid, in a random alloy or in a glass, with slow dynamics, on the other hand, the duration of the exposure is not so relevant, but a source with a high degree of partial coherence can here also reveal a speckle pattern encoding local fluctuations in orientation or ordering.

Due to high penetration of X-rays, multiple scattering effects on a disordered sample of few microns size can be safely neglected and kinematical scattering will be assumed to be valid. This is a very important simplification of the theory that is valid only for a limited number of samples studied by visible light or by electrons, where multiple scattering effects can seldom be neglected. This makes X-rays especially attractive for the study of disordered systems. A low-noise, high-dynamic range detector, with sufficient angular resolution, is also needed to record meaningful angular anisotropies. The very recent emergence of X-ray free-electron lasers (XFELs) [8–10], with ultrabright pulses of few femtoseconds duration and a high degree of transverse coherence, is opening up the promise of a completely new set of experimental conditions and provides further motivation for exploring the potential benefits of correlation analysis.

The revival of angular correlation studies was recently prompted by the work of Wochner et al. [11], which reported angular correlations with pronounced periodic character in a colloidal suspension of polymethylmethacrylate (PMMA) spheres, expected to form icosahedral clusters near the glass formation concentration. They considered angular averages in the form of a cross-correlation function (CCF) calculated on the same scattering ring ($|q_1| = |q_2| = q$) and at the same time $t = t'$ (the scattering vector $\mathbf{q}$, in the plane normal to the incoming beam, being expressed as $\mathbf{q} \equiv (q, \varphi)$)

$$C(q, \Delta) = \frac{\left\langle \widetilde{I}(q, \varphi) \widetilde{I}(q, \varphi + \Delta) \right\rangle_{\varphi}}{\langle I(q, \varphi) \rangle_{\varphi}^2}, \tag{2}$$

where $0 \leq \Delta \leq 2\pi$ is the angular coordinate, $\widetilde{I}(q, \varphi) = I(q, \varphi) - \langle I(q, \varphi) \rangle_{\varphi}$ is the intensity fluctuation, function, and $\langle f(\varphi) \rangle_{\varphi} = (1/2\pi) \int_0^{2\pi} f(\varphi) d\varphi$ denotes the average over the angle φ. This work stimulated further theoretical [12–21] and experimental [22–31] exploration of the CCFs in the studies of disordered materials by X-ray scattering, as well as light [32] and electron scattering [33].

There are two main scientific drivers for the investigation of the angular correlations of X-ray scattering patterns. On the one hand, the angular correlations in scattering experiments are investigated *as a possible tool to solve structures of molecules in solutions* or, more generally, in noncrystalline systems (see Fig. 1). This line of thought, as we saw, goes back to the work of Kam [3], almost 40 years ago; his seminal (although so far not yet implemented in full) idea, was that the intensity fluctuations contain additional information, with respect to the average around the scattering intensity rings. This could allow to go beyond the quantities traditionally extracted from the isotropic patterns (average pair correlation functions in a liquid, or radius of gyrations for molecules in solutions, etc.), possibly all the way to the high-resolution molecular structure. In the more recent applications, the progress in instrumentation opens the door to a rapid acquisition of many scattering patterns; this makes acquisition of angular correlations not only in each diffraction pattern but also over an ensemble of many diffraction patterns possible [3, 34].

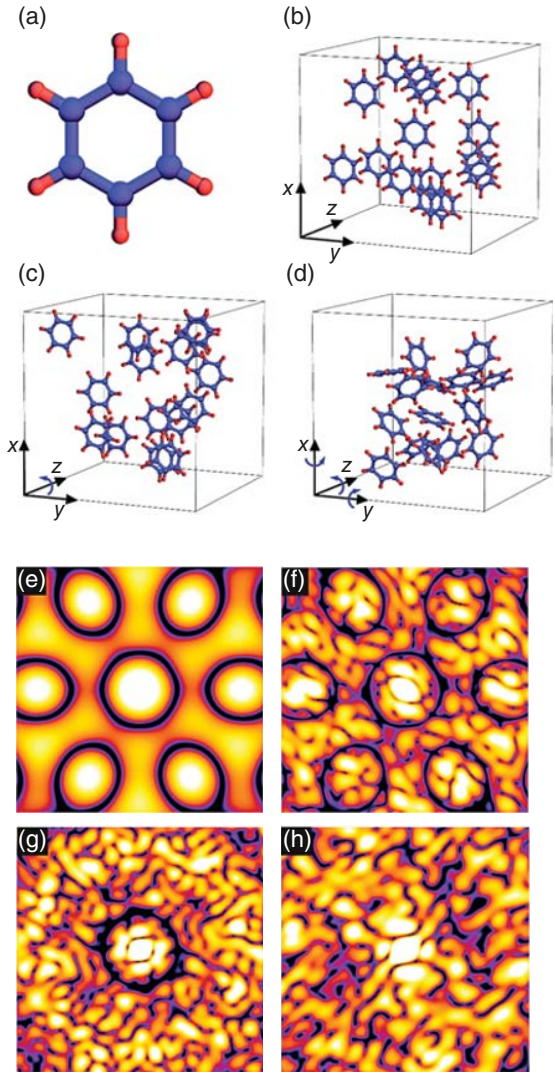

Figure 1. Different types of structural disorder in a system of particles recorded by coherent X-ray snapshots. (a) A single benzene-like molecule and the corresponding simulated coherent diffraction pattern (e). (b) Oriented system of molecules, where particles have random positions but the same orientation as the molecule shown in (a). Corresponding scattering pattern (f) encodes information about a single-particle structure (compare with (e)), modulated by coherent superposition of waves scattered from molecules in different positions. (c) Aligned system of molecules, where in addition to positional disorder particles have random orientations about z-axis. Only the central part of the respective scattering pattern (g) reminds about the single-molecule diffraction pattern (a). (d) Completely disordered system of molecules, where particles have random positions and orientations. Scattering pattern simulated for this system can not be directly associated with the single molecule. In all simulations direction of the incoming beam is assumed along z-axis. (*See insert for color representation of the figure*.)

On the other hand, an alternative application of angular correlations could be very important for the physics of disordered or partially ordered systems: *it is the unveiling of hidden symmetries and of partial order*. This includes systems displaying short-range order (SRO) [35, 36], as well as complicated dynamics, aging, dynamical heterogeneity, and medium-range order (MRO) in a large class of glass-forming liquids [37–41]. In such systems, a relevant question is, for example, if one can recognize and identify an n-fold symmetry axis of an individual molecular species from the diffraction patterns of a liquid composed of such molecules, can bond angles be detected from the study of angular fluctuations of the diffracted intensity of an amorphous system? Encouraging results were in fact obtained in the study of partially ordered quasi two-dimensional (2D) systems, like liquid crystals [42–45] in which hexatic bond-orientational (BO) order can be detected by the study of the angular dependence of the diffracted intensity. More generally, the study of BO order, characterized by the order parameter quantitatively defined in the pioneering work of Steinhardt et al. [35], is also an obvious target for the study of angular correlations.

The structure of this Chapter is as follows. A basic theoretical description of quantities related to angular correlations in a simple X-ray scattering description in the far-field, or Fraunhofer, limit of diffraction in the kinematic approximation is given in Section II. Despite these simplifying assumptions, this analysis shall allow us to draw general conclusions on the nature of the measured correlation functions, on the role of the coherence length of the incoming X-rays, and of the dilution of the physical system under investigation; and to investigate possible approaches toward the two main scientific target areas outlined above for such studies. In Section III, a survey of recent numerical and experimental work is critically discussed. In Section IV, we provide a summary and outlook of the angular cross-correlation methods and their future applications.

II. THEORY

A. Scattering from a Disordered System of Reproducible Particles

We will consider in the following a scattering experiment in transmission geometry as shown in Figure 2a. An incident coherent X-ray beam scatters from a disordered sample, and the resulting speckle pattern is measured on a 2D detector in the far-field. As a general model system, we consider a 3D sample consisting of N identical particles with random positions and orientations (see Fig. 2). The particles itself could, in principle, represent a complicated but reproducible structure. This model includes a variety of systems, for example, clusters or molecules in the gas phase, local structures formed in colloidal systems, viruses in solution, etc.

The amplitude $A_k(\mathbf{q})$ scattered from the k-th particle at the momentum transfer vector $\mathbf{q}$ can be defined as [47]

$$A_k(\mathbf{q}) = \int \rho_k(\mathbf{r}) e^{i\mathbf{q}\cdot\mathbf{r}} d\mathbf{r}, \tag{3}$$

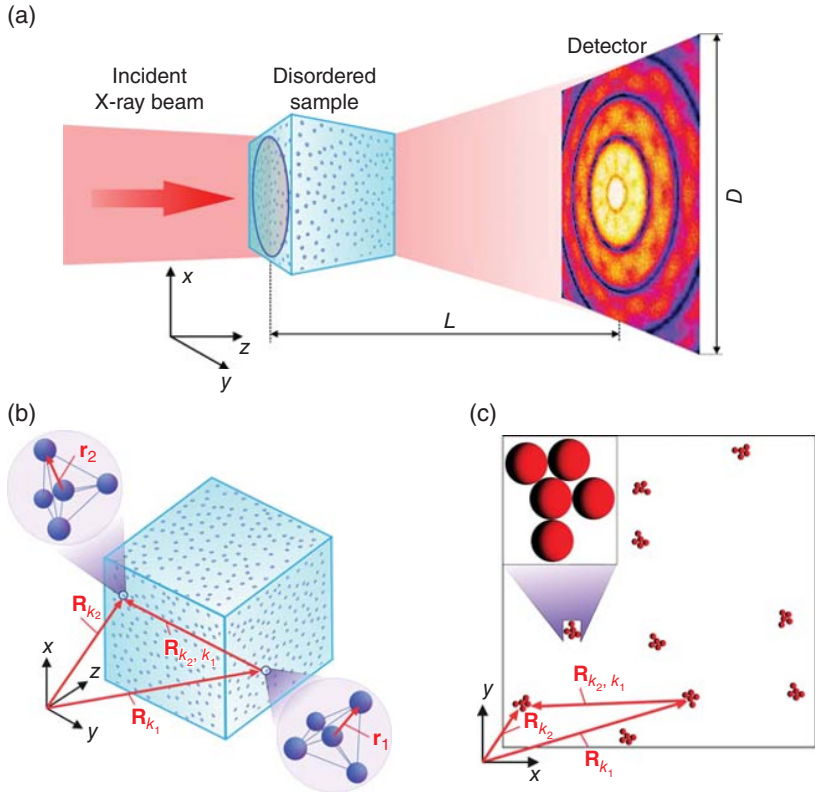

Figure 2. (a) Geometry of the diffraction experiment. A coherent X-ray beam illuminates a disordered sample and produces a diffraction pattern on a detector. The direction of the incident beam is defined along the z-axis of the coordinate system. (b) A disordered 3D sample composed of tetrahedral pentamers. All clusters have random position and orientation in the 3D space. (c) A disordered 2D sample composed of asymmetric clusters. All clusters have random position and orientation in the 2D plane. Reproduced from Ref. 46. Used under CC By 3.0, http://creativecommons.org/licenses/by/3.0/.

where $\rho_k(\mathbf{r})$ is an electron density of the k-th particle (see Fig. 2b) and the integration is performed over the volume of the particle. Using Eq. (3), the intensity $I(\mathbf{q})$ coherently scattered from a disordered sample consisting of N particles at the position $\mathbf{R}_k$ is given by

$$I(\mathbf{q}) = \sum_{k_1,k_2=1}^{N} e^{i\mathbf{q}\cdot\mathbf{R}_{k_2,k_1}} A^*_{k_1}(\mathbf{q}) A_{k_2}(\mathbf{q})$$
$$= \sum_{k_1,k_2=1}^{N} \int\int \rho^*_{k_1}(\mathbf{r}_1)\rho_{k_2}(\mathbf{r}_2) e^{i\mathbf{q}\cdot\mathbf{R}^{21}_{k_2,k_1}} d\mathbf{r}_1 d\mathbf{r}_2, \qquad (4)$$

where the double summation is performed over all N particles, and the integration is performed over the volume of the k_i-th particle ($i = 1, 2$). Here, the following notation for the radius vectors is used, $\mathbf{R}^{21}_{k_2,k_1} = \mathbf{R}_{k_2,k_1} + \mathbf{r}_{21}$, where $\mathbf{R}_{k_2,k_1} = \mathbf{R}_{k_2} - \mathbf{R}_{k_1}$ is the vector connecting two different particles k_1 and k_2, and $\mathbf{r}_{21} = \mathbf{r}_2 - \mathbf{r}_1$, where the vectors $\mathbf{r}_1$ and $\mathbf{r}_2$ are local coordinates inside the particles k_1 and k_2, respectively (see Fig. 2b and c).

In the case of a partially coherent illumination and a dilute disordered system when the mean distance between the particles is larger than the coherence length of the incoming beam, the interparticle correlations due to coherent interference of scattered amplitudes from the individual particles in Eq. (4) can be neglected. In these conditions, the total scattered intensity $I(\mathbf{q})$ can be represented as a sum of intensities $I_k(\mathbf{q}) = |A_k(\mathbf{q})|^2$ corresponding to individual particles in the system

$$I(\mathbf{q}) = \sum_{k=1}^{N} I_k(\mathbf{q}). \tag{5}$$

In the following, we will use Fourier decomposition of the scattered intensity $I(q, \varphi)$ on the ring of radius q (see Fig. 3a),

$$I(q, \varphi) = \sum_{n=-\infty}^{\infty} I_q^n e^{in\varphi}, \tag{6a}$$

$$I_q^n = \frac{1}{2\pi} \int_0^{2\pi} I(q, \varphi) e^{-in\varphi} d\varphi, \tag{6b}$$

where I_q^n are the components of the Fourier decomposition. Since scattered intensities are always real quantities, it is easy to show that $I_q^{-n} = I_q^{n*}$. By its definition, the 0th-order Fourier component represents an angular averaged intensity, $I_q^0 = \langle I(q, \varphi) \rangle_\varphi$.

Here, we would like to note that different authors are using different basic functions for decomposition of the scattered intensities. These are, for example, spherical harmonics [3, 25, 34, 48–52], icosahedral harmonics [15], and 3D Zernike polynomials [17, 53]. The choice of decomposition is often dictated by the symmetry of particles and helps to reduce the number of variables, or unknown parameters.

B. 2D Disordered Systems

In this section, we consider the particular case of a 2D system in a small-angle scattering geometry with a flat Ewald sphere, when all coordinate vectors are defined in a 2D plane (see Fig. 2c), and the electron density of the k-th particle transforms to a projected electron density, $\widetilde{\rho}_k(\mathbf{r}) = \int \rho_k(\mathbf{r}, z) dz$. We would like to note here that in the case of plane wavefront illumination of a 2D system, only even ($n = 2l, l = 1, 2, 3, \ldots$) Fourier components of the intensity I_q^n can have nonzero values [12, 13].

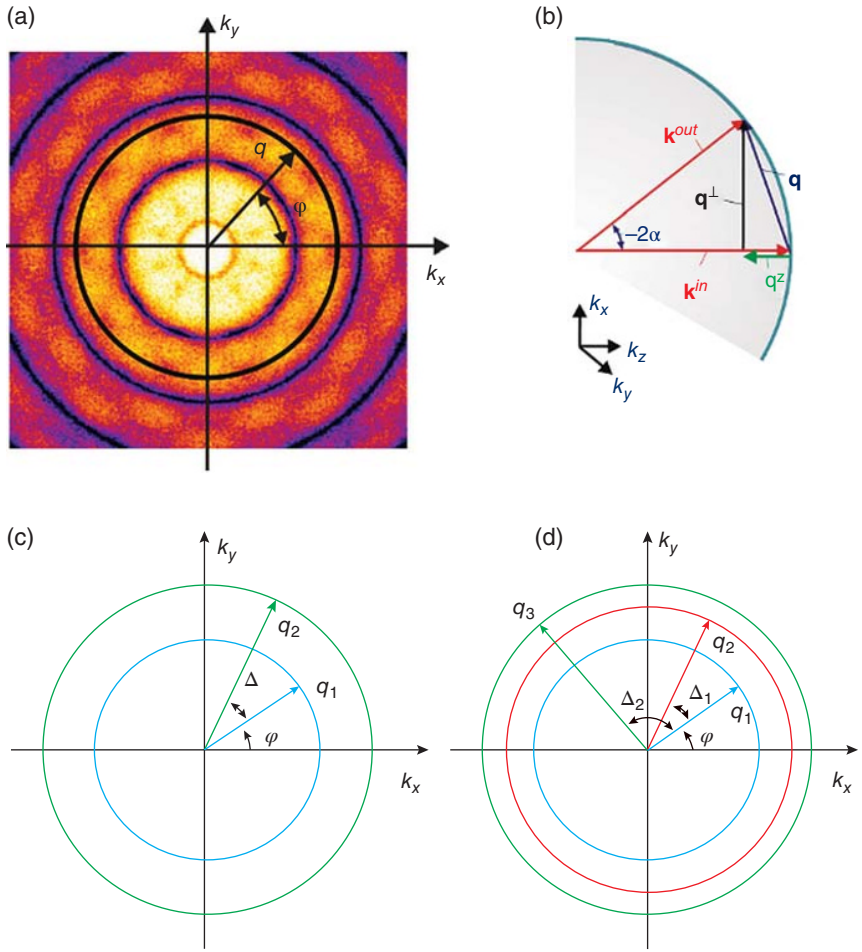

Figure 3. Scattering geometry in reciprocal space. (a) Scattered intensity $I(\mathbf{q})$ defined in the detector plane in the polar coordinate system, $\mathbf{q} = (q, \varphi)$. (b) Ewald sphere construction. Here, $\mathbf{k}^{in}$ is the wavevector of the incident beam directed along the z-axis, $\mathbf{k}^{out}$ is the wavevector of the scattered wave with the scattering angle 2α. The scattering vector $\mathbf{q} = (\mathbf{q}^{\perp}, q^z)$ is decomposed into two components that are perpendicular $\mathbf{q}^{\perp}$ and parallel q^z to the direction of the incident beam. (c and d) Momentum transfer vectors used in the definition of the two-point $C(q_1, q_2, \Delta)$ (c), and three-point CCFs $C(q_1, q_2, q_3, \Delta_1, \Delta_2)$ (d). Reproduced from Ref. 46. Used under CC By 3.0, http://creativecommons.org/licenses/by/3.0/.

1. Dilute Systems

First, we consider scattering from a single particle in a disordered system. The intensity $I_{\psi_0}(\mathbf{q})$ scattered from such a particle in some reference orientation ψ_0 is related to the projected electron density of the particle $\widetilde{\rho}_{\psi_0}(\mathbf{r})$ through its scattered amplitude (Eq. 3) as $I_{\psi_0}(\mathbf{q}) = |A_{\psi_0}(\mathbf{q})|^2$. Similar to $I(\mathbf{q})$ (see Eq. 6a and b), the intensity $I_{\psi_0}(\mathbf{q}) \equiv I_{\psi_0}(q, \varphi)$ can be represented as an angular Fourier series expansion,

$$I_{\psi_0}(q, \varphi) = \sum_{n=-\infty}^{\infty} I^n_{q,\psi_0} e^{in\varphi}, \tag{7}$$

where I^n_{q,ψ_0} are the Fourier components of $I_{\psi_0}(q, \varphi)$.

The Fourier component I^n_{q,ψ_0} is related to the projected electron density $\widetilde{\rho}_{\psi_0}(\mathbf{r})$ of the particle as [12, 13, 16]

$$I^n_{q,\psi_0} = \int\int \widetilde{\rho}^*_{\psi_0}(\mathbf{r}_1)\widetilde{\rho}_{\psi_0}(\mathbf{r}_2) J_n(q|\mathbf{r}_{21}|) e^{-in\phi_{\mathbf{r}_{21}}} d\mathbf{r}_1 d\mathbf{r}_2, \tag{8}$$

where $\phi_{\mathbf{r}_{21}}$ is the angle of the vector $\mathbf{r}_{21}$ in the detector plane, $J_n(\rho)$ is the Bessel function of the first kind of integer order n, and the integration is performed over the area of a particle. According to the structure of I^n_{q,ψ_0}, its value strongly depends on the symmetry of a particle.

The intensity $I_{\psi_k}(q, \varphi)$ scattered from a particle in an arbitrary orientation ψ_k is related to the intensity $I_{\psi_0}(q, \varphi)$ scattered from a particle in the reference orientation ψ_0 (we assume in the following without loss of generality that $\psi_0 = 0$) as $I_{\psi_k}(q, \varphi) = I_{\psi_0}(q, \varphi - \psi_k)$. Applying the shift theorem for the Fourier transforms [55], we obtain for the corresponding Fourier components of the intensities, $I^n_{q,\psi_k} = I^n_{q,\psi_0} \exp(-in\psi_k)$. Using these relations, for a dilute 2D system of identical particles, we can write for the Fourier components I^n_q of the intensity $I(q, \varphi)$ scattered from N particles (Eq. 5)

$$I^n_q = I^n_{q,\psi_0} \sum_{k=1}^{N} e^{-in\psi_k} = I^n_{q,\psi_0} \mathbf{A}_n, \tag{9}$$

where $\mathbf{A}_n = \sum_{k=1}^{N} \exp(-in\psi_k)$ is a random phasor sum [56]. Equation (9) leads to the following expression for the small-angle X-ray scattering (SAXS) intensity, $\langle I(q, \varphi)\rangle_\varphi = N I^0_{q,\psi_0}$.

2. Dense Systems

In the case of a dense system, when the average distance between particles is of the order of the size of a single cluster, the Fourier components I^n_q of the intensity $I(\mathbf{q})$ (Eq. 4) can contain a substantial interparticle contribution.

In this case, I^n_q can be presented as a sum of two terms as follows:

$$I^n_q = I^n_{\mathrm{sp}}(q) + I^n_{\mathrm{ip}}(q). \tag{10}$$

Here $I^n_{\rm sp}(q)$ is attributed to a single-particle structure discussed before, and $I^n_{\rm ip}(q)$ is defined by the interparticle correlations [12, 13, 16]. In a 2D system, these two terms are [12, 13, 16]

$$I^n_{\rm sp}(q) = I^n_{q,\psi_0}\mathbf{A}_n, \tag{11a}$$

$$I^n_{\rm ip}(q) = 2\sum_{k_2>k_1}\int\int \widetilde{\rho}^*_{k_1}(\mathbf{r}_1)\widetilde{\rho}_{k_2}(\mathbf{r}_2)J_n(q|\mathbf{R}^{21}_{k_2,k_1}|)e^{-in\phi_{\mathbf{R}^{21}_{k_2,k_1}}}d\mathbf{r}_1 d\mathbf{r}_2, \tag{11b}$$

where $\phi_{\mathbf{R}^{21}_{k_2,k_1}}$ is the angle of the vector $\mathbf{R}^{21}_{k_2,k_1}$ in the sample plane.

C. 3D Disordered Systems

Here, we consider a general case of 3D systems in which one or more particles are distributed with random positions and orientations in 3D space. In the case of 3D systems nonzero odd Fourier components can be also present when scattering to high angles is considered, due to the effects of Ewald sphere curvature.

In general, the scattering vector $\mathbf{q} = (\mathbf{q}^\perp, q^z)$ can be decomposed into two components: (1) $\mathbf{q}^\perp$ that is perpendicular and (2) q^z that is parallel to the direction of the incident beam (see Fig. 3b). We also define the perpendicular $\mathbf{R}^{\perp 21}_{k_2,k_1} = \mathbf{R}^\perp_{k_2,k_1} + \mathbf{r}^\perp_{21}$, and the z-components $Z^{21}_{k_2,k_1} = Z_{k_2,k_1} + z_{21}$ of the radius vectors (see Figs. 2a and 3). Using these notations we can write Eq. (4) in the following form:

$$I(\mathbf{q}) = \sum_{k_1,k_2=1}^{N} e^{-iq^z\cdot Z_{k_2,k_1}}\int\int \widetilde{\rho}^*_{k_1}(\mathbf{r}^\perp_1, q^z)\widetilde{\rho}_{k_2}(\mathbf{r}^\perp_2, q^z)e^{i\mathbf{q}^\perp\cdot\mathbf{R}^{\perp 21}_{k_2,k_1}}d\mathbf{r}^\perp_1 d\mathbf{r}^\perp_2. \tag{12}$$

Here, we introduced a modified complex valued electron density function, defined as follows:

$$\widetilde{\rho}_{k_i}(\mathbf{r}^\perp_i, q^z) = \int \rho_{k_i}(\mathbf{r}^\perp_i, z)e^{-iq^z z}dz. \tag{13}$$

In the case of wide-angle scattering, the effect of the Ewald sphere curvature (see Fig. 3b), which manifests itself by the presence of the exponential factors $e^{-iq^z\cdot Z_{k_2,k_1}}$ and $e^{-iq^z z}$ in Eqs. (12) and (13), may become important. This effect can break the scattering symmetry of a diffraction pattern, characteristic for the scattering on a positive valued electron density (Friedel's law) and may help to reveal symmetries that cannot be directly observed in the small-angle scattering case. A wide-angle scattering geometry may become important for scattering on atomic systems with local interatomic distances of the order of few Ångstroms.

For simplicity, we will consider here a 3D system consisting of particles composed of isotropical identical scatterers. The modified electron density

of a particle according to Eq. (13) can be represented in the following form [7]:

$$\widetilde{\rho}_k(\mathbf{r}^{\perp}, q^z) = f(q) \sum_{i=1}^{N_s} \delta(\mathbf{r}^{\perp} - \mathbf{r}_i^{\perp}) e^{-iq^z z_i}. \tag{14}$$

Here $f(q)$ is a form-factor of a scatterer, and N_s is a number of scatterers in the cluster. The coordinates $(\mathbf{r}_i^{\perp}, z_i)$ define the position of the i-th scatterer inside the k-th cluster. Using this definition and performing Fourier transformation of Eq. (12), we obtain for the Fourier coefficients of intensity [12, 13]

$$I^n(q^{\perp}, q^z) = (i)^n |f(q)|^2 \sum_{k_1,k_2=1}^{N} \sum_{l,m=1}^{N_s} e^{-iq^z Z^{ml}_{k_2,k_1}} J_n(|\mathbf{q}^{\perp}| \cdot |\mathbf{R}^{\perp ml}_{k_2,k_1}|) e^{-in\phi_{\mathbf{R}^{\perp ml}_{k_2,k_1}}}, \tag{15}$$

where the summation over index l is performed over the positions of scatterers in the cluster k_1, and the summation over index m is performed over the positions of scatterers in the cluster k_2. We note here that due to the property of the Bessel functions [$J_n(0) = 0$ for $n \neq 0$], the terms with $k_1 = k_2$ and $l = m$ are equal to zero. Taking into account that the terms with interchanged indices, that is, k_1, k_2 and k_2, k_1, as well as l, m and m, l, differ from each other by a change of the sign of $Z^{ml}_{k_2,k_1}$ and by an additional factor $(-1)^n$, which arises due to the change of the phase $\phi_{\mathbf{R}^{\perp ml}_{k_2,k_1}} = \phi_{\mathbf{R}^{\perp lm}_{k_1,k_2}} + \pi$, we have the following for *even* values of n in Eq. (15) [12, 13]:

$$\begin{aligned} &I^n(q^{\perp}, q^z) \\ &= 2(i)^n |f(q)|^2 \left[\sum_{\substack{1 \le k_1 \le N \\ k_1 < k_2 \le N}} \sum_{\substack{1 \le l \le N_s \\ 1 \le m \le N_s}} \cos(q^z Z^{ml}_{k_2,k_1}) J_n(|\mathbf{q}^{\perp}| \cdot |\mathbf{R}^{\perp ml}_{k_2,k_1}|) e^{-in\phi_{\mathbf{R}^{\perp ml}_{k_2,k_1}}} \right. \\ &\quad \left. + \sum_{1 \le k \le N} \sum_{\substack{1 \le l \le N_s \\ l \le m \le N_s}} \cos(q^z Z^{ml}_{k}) J_n(|\mathbf{q}^{\perp}| \cdot |\mathbf{R}^{\perp ml}_{k}|) e^{-in\phi_{\mathbf{R}^{\perp ml}_{k}}} \right]. \end{aligned} \tag{16}$$

For *odd* values of n,

$$\begin{aligned} &I^n(q^{\perp}, q^z) \\ &= -2(i)^{n+1} |f(q)|^2 \left[\sum_{\substack{1 \le k_1 \le N \\ k_1 < k_2 \le N}} \sum_{\substack{1 \le l \le N_s \\ 1 \le m \le N_s}} \sin(q^z Z^{ml}_{k_2,k_1}) J_n(|\mathbf{q}^{\perp}| \cdot |\mathbf{R}^{\perp ml}_{k_2,k_1}|) e^{-in\phi_{\mathbf{R}^{\perp ml}_{k_2,k_1}}} \right. \\ &\quad \left. + \sum_{1 \le k \le N} \sum_{\substack{1 \le l \le N_s \\ l \le m \le N_s}} \sin(q^z Z^{ml}_{k}) J_n(|\mathbf{q}^{\perp}| \cdot |\mathbf{R}^{\perp ml}_{k}|) e^{-in\phi_{\mathbf{R}^{\perp ml}_{k}}} \right], \end{aligned} \tag{17}$$

where $\mathbf{R}_k^{\perp ml} = \mathbf{R}_{k,k}^{\perp ml}$ and $Z_k^{ml} = Z_{k,k}^{ml}$. From the performed analysis, we can see that, due to the curvature of the Ewald sphere (nonzero q^z component), we obtain nonzero odd Fourier components of the CCF when scattering from a 3D system. These components become negligibly small for experimental conditions corresponding to a flat Ewald sphere, considered in Section II.B.

In the case of a dilute sample, the Fourier components of intensity defined in Eq. (14) reduce to

$$I^n(q^\perp, q^z) = (i)^n |f(q)|^2 \sum_{k=1}^{N} \sum_{l,m=1}^{N_s} e^{-iq^z z_k^{ml}} J_n(|\mathbf{q}^\perp| \cdot |\mathbf{r}_k^{\perp ml}|) e^{-in\phi_{\mathbf{r}_k^{\perp ml}}}. \tag{18}$$

Here, we would like to note that if in a 3D system all particles are aligned (as in Fig. 1b) or rotated around a single axis parallel to the incoming beam (Fig. 1c), and conditions of small-angle scattering are satisfied ($q_z \simeq 0$), then the analysis of scattering can be performed in the same way as for a 2D system described in Section II.B.

D. Two- and Three-Point Angular CCFs and Their Fourier Decomposition

1. General Definitions

The two-point CCF defined for a single realization of a disordered system at two resolution rings, q_1 and q_2, is given by [3, 12, 13, 57] (see Fig. 3c)

$$C(q_1, q_2, \Delta) = \left\langle \widetilde{I}(q_1, \varphi) \widetilde{I}(q_2, \varphi + \Delta) \right\rangle_\varphi, \tag{19}$$

where $0 \le \Delta \le 2\pi$ is the angular coordinate, $\widetilde{I}(q, \varphi) = I(q, \varphi) - \langle I(q, \varphi) \rangle_\varphi$ is the intensity fluctuation function, and $\langle f(\varphi) \rangle_\varphi = (1/2\pi) \int_0^{2\pi} f(\varphi) d\varphi$ denotes the average over the angle φ. We should note here that due to fluctuations of intensity on a pulsed sources as XFELs, the normalized intensity should be used in Eq. (19). In practice, we used normalization to the integrated intensity measured on the detector from each pulse.

In a similar way, the three-point CCF for a single realization of a system is defined at three resolution rings, q_1, q_2, and q_3, as [3, 18] (see Fig. 3d) as follows:

$$C(q_1, q_2, q_3, \Delta_1, \Delta_2) = \left\langle \widetilde{I}(q_1, \varphi) \widetilde{I}(q_2, \varphi + \Delta_1) \widetilde{I}(q_3, \varphi + \Delta_2) \right\rangle_\varphi. \tag{20}$$

Here $0 \le \Delta_1 \le 2\pi$ and $0 \le \Delta_2 \le 2\pi$ are the angular coordinates.

It is convenient to analyze CCFs using a Fourier series decomposition in the $(0, 2\pi)$ interval [12, 13]. In the case of the two-point CCF $C(q_1, q_2, \Delta)$, it gives

$$C(q_1, q_2, \Delta) = \sum_{n=-\infty}^{\infty} C^n_{q_1,q_2} e^{in\Delta}, \tag{21a}$$

$$C^n_{q_1,q_2} = \frac{1}{2\pi} \int_0^{2\pi} C(q_1, q_2, \Delta) e^{-in\Delta} d\Delta. \tag{21b}$$

Here, $C^n_{q_1,q_2}$ is the n-th component in the Fourier series expansion of $C(q_1, q_2, \Delta)$, and $C^0_{q_1,q_2} = 0$ at $n = 0$ by definition (see Eq. 19). Substituting Eq. (19) into Eq. (21b) and applying the Fourier convolution theorem, we get the following:

$$C^n_{q_1,q_2} = I^{n*}_{q_1} \cdot I^n_{q_2}. \tag{22}$$

Here, I^n_q are the components of the Fourier expansion of the scattered intensity $I(q, \varphi)$ defined in (6b). As soon as $I^{-n}_q = I^{n*}_q$, we obtain for the Fourier components of CCFs and $C^{-n}_{q_1,q_2} = C^{n*}_{q_1,q_2}$.

In the specific case, when $q_1 = q_2 = q$, Eqs. (21a) and (22) reduce to

$$C(q, \Delta) = 2 \sum_{n=1}^{\infty} C^n_q \cos(n\Delta), \tag{23a}$$

$$C^n_q = |I^n_q|^2, \quad C^n_q \geq 0. \tag{23b}$$

According to (23a), a strong single cosine dependence of $C(q, \Delta)$ can be observed for those values of q, at which one of the Fourier components C^n_q significantly dominates over all others [11]. Such components can be related to the structure and symmetry of the system [12, 13, 16].

The Fourier series expansion of the three-point CCF $C(q_1, q_2, q_3, \Delta_1, \Delta_2)$ can be written as follows:

$$C(q_1, q_2, q_3, \Delta_1, \Delta_2) = \sum_{n_1=-\infty}^{\infty} \sum_{n_2=-\infty}^{\infty} C^{n_1,n_2}_{q_1,q_2,q_3} e^{in_1\Delta_1} e^{in_2\Delta_2}, \tag{24a}$$

$$C^{n_1,n_2}_{q_1,q_2,q_3} = \left(\frac{1}{2\pi}\right)^2 \int_0^{2\pi} \int_0^{2\pi} C(q_1, q_2, q_3, \Delta_1, \Delta_2) e^{-in_1\Delta_1} e^{-in_2\Delta_2} d\Delta_1 d\Delta_2. \tag{24b}$$

Here $C^{n_1,n_2}_{q_1,q_2,q_3}$ are the Fourier components of the three-point CCF, and $C^{n_1,n_2}_{q_1,q_2,q_3} = 0$ for $n_1 = 0$, $n_2 = 0$, and $n_1 = -n_2$. Substituting Eq. (20) into Eq. (24b), one can get the following [18]:

$$C^{n_1,n_2}_{q_1,q_2,q_3} = I^{(n_1+n_2)*}_{q_1} I^{n_1}_{q_2} I^{n_2}_{q_3}. \tag{25}$$

In general, Eq. (25) determines a relation between three different Fourier components of intensity I^n_q of the order n_1, n_2 and $n_1 + n_2$, defined on three resolution rings, q_1, q_2, and q_3.

In practical applications, one would need to consider CCFs and Fourier components of CCFs averaged over a sufficiently large number M of diffraction patterns [16, 18]. Such averaging can be defined as a general rule

$$\langle C \rangle_M = 1/M \sum_{m=1}^{M} C_m, \tag{26}$$

where C is one of the quantities $C(q_1, q_2, \Delta)$, $C(q_1, q_2, q_3, \Delta_1, \Delta_2)$, $C^n_{q_1,q_2}$, or $C^{n_1,n_2}_{q_1,q_2,q_3}$ and C_m is defined for the m-th realization of a disordered system.

The analysis presented here shows that in the Fourier domain, the two-point angular intensity CCF reduces to a product of two Fourier components of intensity (see Eq. 22). Similarly in the case of the three-point CCF, we obtain a product of three Fourier components of intensity (see Eq. 25). Taking into account that intensity distribution itself gives information on density–density (or pair correlation) functions, it means that the angular XCCA may be considered as a particular case of the higher order correlation functions [12, 13]. However, the general question of revealing the higher order correlation functions of an arbitrary form in disordered systems [58] by means of cross-correlation approaches remains open.

2. *Analysis of Disordered Systems by Angular CCFs*

Substituting Eq. (9) in Eq. (22) in the limit of dilute systems, we have for the Fourier components $C^n_{q_1,q_2}$ of the CCF the following expression:

$$C^n_{q_1,q_2} = I^{n*}_{q_1,\psi_0} I^n_{q_2,\psi_0} |\mathbf{A}_n|^2 . \tag{27}$$

The statistical behavior of $\mathbf{A}_n$ has been analyzed for different angular distributions of orientations of particles in the system (see Refs. 12, 13 and 16). It is clear that in the case of a completely oriented system of particles (all $\psi_k = 0$), the square amplitude of the random phasor sum $|\mathbf{A}_n|^2$ is equal to N and $C^n_{q_1,q_2} = N I^{n*}_{q_1,\psi_0} I^n_{q_2,\psi_0}$. In the case of a uniform distribution of orientations of particles, $|\mathbf{A}_n|^2$ fluctuates around its mean value $\langle |\mathbf{A}_n|^2 \rangle_M = N$ with the standard deviation $\sigma_{|\mathbf{A}_n|^2} = N$. Averaging the Fourier components $C^n_{q_1,q_2}$ over a large number M of diffraction patterns leads to the following asymptotic result: [12, 13, 16]

$$\left\langle C^n_{q_1,q_2} \right\rangle_M = I^{n*}_{q_1,\psi_0} I^n_{q_2,\psi_0} \cdot \left\langle |\mathbf{A}_n|^2 \right\rangle_M \underset{M\to\infty}{\longrightarrow} N I^{n*}_{q_1,\psi_0} I^n_{q_2,\psi_0}. \tag{28}$$

Here $\langle \cdots \rangle_M$ denotes statistical averaging over M diffraction patterns. Importantly, the ensemble-averaged Fourier components $\langle C^n_{q_1,q_2} \rangle_M$ converge to a scaled product of the two Fourier components of intensity $I^{n*}_{q_1,\psi_0}$ and $I^n_{q_2,\psi_0}$ associated with a single particle.

Using the approach developed before, it is possible to determine the amplitudes $|I^n_{q,\psi_0}|$ and phases ϕ^n_{q,ψ_0} (for $n \neq 0$) of the Fourier components

$I^n_{q,\psi_0} = |I^n_{q,\psi_0}| \exp(i\phi^n_{q,\psi_0})$ associated with a single particle. They can be obtained using Eq. (28) [18]. This equation gives the phase difference between two Fourier components $I^n_{q_1,\psi_0}$ and $I^n_{q_2,\psi_0}$ of the same order n, defined at two different resolution rings, q_1 and q_2,

$$\arg\left[\left\langle C^n_{q_1,q_2}\right\rangle_M\right] = \phi^n_{q_2,\psi_0} - \phi^n_{q_1,\psi_0}. \tag{29}$$

Similar to the Fourier components of the two-point CCF, the Fourier components of the three-point CCF equation (25) can be expressed in the limit of a dilute system as follows: [18]

$$C^{n_1,n_2}_{q_1,q_2,q_3} = I^{(n_1+n_2)*}_{q_1,\psi_0} I^{n_1}_{q_2,\psi_0} I^{n_2}_{q_3,\psi_0} \cdot \mathbf{A}_{n_1,n_2}, \tag{30}$$

Here $\mathbf{A}_{n_1,n_2} = \sum_{i,j,k=1}^{N} \exp\{i[(n_1+n_2)\psi_i - n_1\psi_j - n_2\psi_k]\}$ is another random phasor sum. Our analysis shows [18] that in the case of a uniform distribution of orientations of N particles, the statistical average $\langle \mathbf{A}_{n_1,n_2}\rangle_M$ converges to N for a sufficiently large number M of diffraction patterns,

$$\left\langle C^{n_1,n_2}_{q_1,q_2,q_3}\right\rangle_M \underset{M\to\infty}{\longrightarrow} N I^{(n_1+n_2)*}_{q_1,\psi_0} I^{n_1}_{q_2,\psi_0} I^{n_2}_{q_3,\psi_0}. \tag{31}$$

An important result of Eq. (31) is that the ensemble-averaged Fourier components $\langle C^{n_1,n_2}_{q_1,q_2,q_3}\rangle_M$ converge to a scaled product of three Fourier components of intensity $I^{(n_1+n_2)*}_{q_1,\psi_0}$, $I^{n_1}_{q_2,\psi_0}$, and $I^{n_2}_{q_3,\psi_0}$ associated with a single particle. Equation (31) also provides the following phase relation:

$$\arg\left[\left\langle C^{n_1,n_2}_{q_1,q_2,q_3}\right\rangle_M\right] = \phi^{n_1}_{q_2,\psi_0} + \phi^{n_2}_{q_3,\psi_0} - \phi^{(n_1+n_2)}_{q_1,\psi_0}. \tag{32}$$

This equation determines the phase difference between three Fourier components $I^{(n_1+n_2)}_{q_1,\psi_0}$, $I^{n_1}_{q_2,\psi_0}$, and $I^{n_2}_{q_3,\psi_0}$ of different order n defined on three resolution rings. If $n_1 = n_2 = n$ and $n_3 = 2n$, Eq. (32) reduces to a particular form, giving the phase relation between Fourier components of only two different orders, n and $2n$. Phase relations (29) and (32) can be used to determine the phases of the complex Fourier components I^n_{q,ψ_0} using measured CCFs from a disordered system of particles [18, 26].

The influence of interparticle correlations on CCFs in dense systems were discussed in detail in Refs. 12 and 16.

III. APPLICATIONS

In this section, we review the applications of the CCFs in X-ray studies of materials divided into two major groups. The first part of applications is related to the problem of a single-particle structure recovery in the fluctuation X-ray scattering (FXS) experiments [3, 14, 17, 18, 21, 24, 26, 46, 50, 57, 59–63]. The second part is related to the studies of structural properties of disordered and partially

ordered systems, such as colloids, metallic glasses, liquid crystals, and polymers. Applications, where CCFs serve as subsidiary mathematical tools and are not directly related to the analysis of material properties, for example, in diffraction pattern classification algorithms [64], or powder diffraction analysis software [65], will not be discussed here. While concentrating mostly on X-ray applications, in particular cases we also refer to the results obtained in electron or light scattering experiments, both to highlight the generality of the cross-correlation approaches and their peculiarities for different techniques.

A. Single-Particle Structure Recovery from FXS

With the emergence of XFELs [8–10], single-particle diffractive imaging experiments became one of the important challenges of materials research [66–68]. The basic idea behind a single-particle experiment is to determine the structure of particles (e.g., macromolecules and viruses) that cannot be crystallized and studied by conventional scattering techniques. While it is expected that using the high-power ultrashort coherent pulses produced by XFELs, the structure of a single particle can be measured before its desintegration by intense radiation [69–73], the practical realization of this idea is still challenging. Complementary techniques that could profit out of the unique properties of XFELs and provide structural information on a single particle have become of great interest.

One of the potential approaches that could resolve this problem is based on the paradigm "scatter from many — determine single" [46], which is directly related to the FXS experiment proposed by Kam [3]. In such an experiment, a limited number of identical particles N in solution is illuminated by the X-ray beam, with the exposure time shorter than the rotational diffusion time of the particles [3]. At the time this experiment was proposed, FXS measurements would ideally require a frozen dilute solution of particles to slow down particle dynamics [59]. Nowadays, this requirement can be realized at modern XFELs, where the sample looks "frozen" to an incident X-ray pulse of femtosecond duration. Such experiment would allow to measure the instantaneous fluctuations of the scattered intensity about the average signal, and to use this information for structure recovery [3, 49, 50, 59]. The advantage of the FXS experiment is that the scattered intensity is N times higher as compared to a single-particle scattering experiment, that is especially attractive for weakly scattering biological particles. Another important advantage is that the particles do not need to be crystallized, as it is required in conventional crystallographic techniques, or modern serial nanocrystallography experiments [74, 75].

Although the problem of single-particle structure determination from FXS is, in general, related to recovery of a 3D structure of a particle, we start with a particular case of 2D structure determination. Here, the term "2D structure" refers to a projection of the electron density of a particle on a certain plain, while "3D structure" means full structure of a particle in 3D space.